Accurate Position Control for Hydraulic Servomechanisms

M. Pencelli[a,b], R. Villa[b], A. Argiolas [a], G. Ferretti[b], M. Niccolini[a], M. Ragaglia[a], P. Rocco[b] and A. M. Zanchettin[b]

[a]Yanmar R&D Europe S.r.l
[b]Politecnico di Milano
E-mail: manuel_pencelli@yanmar.com, renzo.villa@polimi.it

Abstract -

A common problem when operating heavy hydraulic machines consists in the inability of performing accurate motion. In the last few years the development of non-linear control techniques and the production of increasingly more accurate and cheaper hydraulic drives induced a steadily growing interest towards the development of controlled hydraulic systems. Clearly, this interest is also motivated by the possibility to exploit the huge power density, which is an intrinsic feature of hydraulic systems. This paper specifically focuses on the development of several position control schemes, whose aim is to guarantee accurate motion of a standalone hydraulic servomechanism. By relying on an experimentally validated mathematical model of the servomechanism itself, different control schemes have been synthesized and the resulting control performances have been verified and compared together.

Keywords -

Hydraulic systems, Hydraulic actuators, Motion Control

1 Introduction

Nowadays the vast majority of high performance servomechanisms is composed by electrical servomechanisms. Nevertheless, hydraulic actuation systems are characterized by multiple convenient features (namely high power density, reliability, and relatively low maintenance cost) that make them particularly fit to several application domains, like for instance: construction and earthworks machinery [1, 2], mining industry [3], agriculture and forestry [4]. Typically, hydraulic servomechanisms are controlled either manually by human operators opening and closing valves, or by using heavily approximated linear controllers.

Specifically in case of linear controllers, obtaining accurate motion of such kind of servomechanisms is a quite complex task, mainly due to the highly non-linear dynamics describing the behaviour of valves, and to high parametric uncertainty affecting the mathematical models of the different system components. Given this situation, the resulting motion is often characterized either by very low accuracy and repeatability or by a limited bandwidth of the closed loop system due to a rather conservative design in order to ensure stability. Despite the mentioned problems, linear controllers are still implemented for hydraulic servomechanism [5] because of their simplicity and the consolidated well-known theoretical background [6].

However, recent research developments in the field of non-linear control finally allowed to overcome some of the aforementioned limitations and to guarantee reasonably good performance. Among these non-linear control strategies, Sliding Mode Control (SMC) is probably the most widespread solution when dealing with hydraulic actuators [7, 8]. More recently, in [9] a 1^{st}-order SMC scheme was applied to control a 1-DoF hydraulic crane, while in [10] a 2^{nd}-order SMC scheme for the same system was proposed. Dynamic switching functions have been introduced in [11] and also adaptive SMC laws have been proposed [12, 13] in order to improve the robustness of the controller of an hydraulic motor. Finally, a comprehensive discussion of the various application of SMC to hydraulic systems is given in [14], while alternative approaches based on backstepping [15] and cascaded adaptive control [16, 17, 18, 19] have also been proposed.

With respect to the mentioned scientific literature, the main contribution of this work consists in an experimentally-based comparative evaluation of the performance levels of an advanced P-PI linear controller and an approximated 1^{st}-order SMC, both applied on a standalone hydraulic servomechanisms. First, the paper details the development and the validation of the mentioned control strategies aiming. Then, a comparative evaluation of the performance of the proposed control strategies is discussed. In particular, starting from a previously validated dynamic model of a generic hydraulic servomechanisms [20], a linear cascade control with static compensation of the dead-zone and a 1^{st}-order SMC have been synthesized. The tracking performance of time-varying reference signals of the SMC scheme has been improved by introducing a model-based feed-forward action. In addition, the high frequency chattering (caused by the SMC action) has been reduced by approximating the discontinuity inside the SMC law with a sigmoid function. Finally, the performance of the different closed-loop control systems have been tested on an experimental test-bench.

The paper is organized as follows. Section 2 briefly introduces the dynamic model of the hydraulic servomechanism, while Section 3 describes the linear controller scheme synthesized on the basis of the linearized dynamic model. Then, Section 4 details the development of the proposed SMC schemes and Section 5 shows the experimental validation of all the proposed control schemes and discusses the performance levels achieved by each solution. Finally, conclusions and future developments are presented in Section 6.

2 Hydraulic Servomechanism Model

The dynamic model of the generic hydraulic servomechanism used as a basis to develop the proposed control algorithms is defined as follows:

$$\begin{cases} \dot{x}_p = \dot{x}_p \\ \ddot{x}_p = \frac{1}{M}[A_1 P_1 - A_2 P_2 - f_r(\dot{x}_p) - D\dot{x}_p - \zeta \dot{x}_p^2 - Mg] \\ \dot{P}_1 = \frac{\beta}{V_1(x_p)}(Q_1 - A_1 \dot{x}_p) \\ \dot{P}_2 = \frac{\beta}{V_1(x_p)}(-Q_2 + A_2 \dot{x}_p) \end{cases} \tag{1}$$

$$Q_1 = \begin{cases} c_1(P_p - P_1) - c_2(P_1 - P_t) & d_z^- < x_v < d_z^+ \\ k_1^+(x_v)\frac{\pi}{4}\frac{d^2 x_v^2}{\sqrt{1-x_v^4}}\sqrt{\frac{2}{\rho}(Pp - P_1)} & x_v \geq d_z^+ \\ -k_1^-(x_v)\frac{\pi}{4}\frac{d^2 x_v^2}{\sqrt{1-x_v^4}}\sqrt{\frac{2}{\rho}(P1 - P_t)} & x_v < d_z^- \end{cases} \tag{2}$$

$$Q_2 = \begin{cases} c_3(P_p - P_2) - c_4(P_2 - P_t) & d_z^- < x_v < d_z^+ \\ k_2^+(x_v)\frac{\pi}{4}\frac{d^2 x_v^2}{\sqrt{1-x_v^4}}\sqrt{\frac{2}{\rho}(Pp - P_2)} & x_v \geq d_z^+ \\ -k_2^-(x_v)\frac{\pi}{4}\frac{d^2 x_v^2}{\sqrt{1-x_v^4}}\sqrt{\frac{2}{\rho}(P_2 - P_t)} & x_v < d_z^- \end{cases} \tag{3}$$

where:

- x_p, $\dot{x}_p$, $\ddot{x}_p$: hydraulic cylinder position, velocity and acceleration, respectively;
- M: mass of the mechanical load;
- A_1, (A_2): bottom(rod)-side chamber internal surfaces;
- V_1, (V_2): bottom(rod)-side chamber internal volumes;
- P_1, (P_2): bottom(rod)-side chamber internal pressures;
- $f_r(\cdot)$: Coulomb friction function;
- D: viscous friction coefficient;
- ζ: dynamic pressure loss coefficient;
- g: gravitational constant;
- β: mineral oil bulk modulus;
- Q_1: flow rate from tank to bottom-side chamber;
- Q_2: flow rate from rod-side chamber to tank;
- c_i: valve static pressure loss coefficients;
- P_p: pump pressure;
- P_t: tank pressure;
- x_v: valve PWM, acting as control signal;
- $k_1^{\pm}(\cdot)$, ($k_2^{\pm}(\cdot)$): bottom(rod)-side chamber valve opening function2;
- d: valve orifice diameter;
- ρ: mineral oil density;
- d_z^-, d_z^+: valve negative and positive dead-zones.

A more detailed discussion of the dynamic model (along with its experimental validation) can be found in [20].

3 Linear Controller

In this Section a linearized version of the previously introduced dynamic model is given, allowing to synthesize a linear control scheme.

3.1 Dynamic Model Linearization

Starting from equations (1)-(3), the linearized model can be computed. The equilibrium point has been chosen by considering the valve opening outside of the deadzone region and by taking the middle position of the cylinder as working point:

$$\begin{aligned} &\overline{x}_v < d_z^- \quad \vee \quad \overline{x}_v > d_z^+ \\ &\overline{x}_p = \frac{{x_p}^{MAX} - x_{p\,min}}{2} \\ &\overline{V}_1 = A_1 \overline{x}_p, \quad \overline{V}_2 = A_2 \overline{x}_p \end{aligned} \tag{4}$$

consequently, the following set of linear equation is obtained:

$$\begin{pmatrix} \delta\ddot{x}_p \\ \delta\dot{P}_1 \\ \delta\dot{P}_2 \end{pmatrix} = \begin{pmatrix} \frac{-(D+2\zeta\dot{x}_p)}{M} & \frac{A_1}{M} & \frac{-A_2}{M} \\ \frac{-\beta A_1}{\bar{V}_1} & \frac{\beta\lambda_1}{\bar{V}_1} & 0 \\ \frac{\beta A_2}{\bar{V}_2} & 0 & \frac{-\beta\lambda_2}{\bar{V}_2} \end{pmatrix} \begin{pmatrix} \delta\dot{x}_p \\ \delta P_1 \\ \delta P_2 \end{pmatrix} + \begin{pmatrix} 0 \\ \frac{\beta\lambda_3}{\bar{V}_1} \\ \frac{-\beta\lambda_4}{\bar{V}_2} \end{pmatrix} \delta x_v \tag{5}$$

where $\lambda_1, \lambda_2, \lambda_3, \lambda_4$ are the linearization coefficients of the valve:

$$\begin{aligned} \delta q_1 &= \lambda_1 \delta P_1 + \lambda_3 \delta x_v \\ \delta q_2 &= \lambda_2 \delta P_2 + \lambda_4 \delta x_v \end{aligned} \tag{6}$$

Finally, the state space formulation can be turned into the corresponding transfer function between the valve opening and the cylinder velocity:

$$F(s) = \frac{\delta \dot{x}_p(s)}{\delta x_v(s)} = k_f \frac{\tau_1 s + 1}{(\tau_2 s + 1)(s^2/\omega^2 + 2Ds/\omega + 1)} \tag{7}$$

and the transfer function between the valve opening and the cylinder position can be obtained by simply integrating the cylinder velocity:

$$G(s) = \frac{\delta x_p(s)}{\delta x_v(s)} = \frac{F(s)}{s} \tag{8}$$

3.2 Controller Block Scheme

After linearization of the dynamic model, the cascaded control scheme has been developed (see Figure 1). A proportional-integral (PI) controller with anti-windup block was chosen for the inner velocity loop, while a pure proportional (P) controller was selected for the outer position loop. On the top left part of the digram it is possible to see a derivative block that outputs a velocity feed-forward term that helps improving tracking performance. On the other hand, since a direct measure of the cylinder velocity is not available, another derivative block is needed in order to indirectly compute $\dot{x}_p$. Clearly, each derivative block is equipped with a tunable low pass filter in order to ensure that the transfer function of the complete system is proper. Moreover, the filter inside the feed-forward derivative block ensures that the control action is not too aggressive, while the one on the measurement line mitigates the effect of the noise. Finally, the saturation blocks ensure that the value of the valve opening stays inside the admissible range $[-1,\ +1]$, while the "*sig*" block contains the dead-zone compensation function $sig\,(u)$, defined as:

$$sig\,(u) = d_z^- + \frac{d_z^+ - d_z^-}{1 + e^{-\eta u}} \tag{9}$$

in order to avoid chattering of the controlled variable. For the sake of completeness, to tune the control gains it is sufficient to neglect the effect of the non-linear blocks and to apply the Bode criterion to both the internal velocity loop and to the external position one.

4 Sliding Mode Controller

The parametric uncertainties and the intrinsic high non-linearities of hydraulic systems can greatly deteriorate the performances of classical linear controllers, especially when the state configuration of the system is far from the linearization point. For this reason SMC can be a suitable alternative for the realization of an accurate position control. In this Section, after a brief overview of the SMC theory is given and the control law adopted for our system is presented and. Finally, the condition that guarantees the overall stability of the closed loop is discussed.

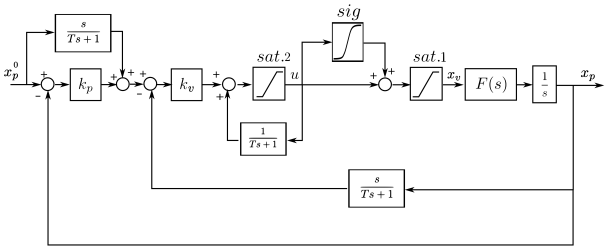

Figure 1. P-PI cascaded control scheme with anti-windup, feed-forward and dead-zone compensation.

4.1 Sliding mode control overview

The main properties of SMC are the robustness with respect to both external disturbances and parametric uncertainties, and the capability to constrain the system state within a specific a-priori defined state subspace. This subspace is called "sliding surface" and it is defined by:

$$S = \{\mathbf{x} : \sigma(\mathbf{x}) = 0\} \tag{10}$$

where $\mathbf{x} \in R^n$ is the state vector of a given system and $\sigma(\mathbf{x}) : R^n \rightarrow R$ is the sliding variable, a function properly defined in order to achieve the desired performances. Given a generic non-linear SISO system with bounded state:

$$|\dot{x}_i| < U_i, \quad |x_i| < Ub_i, \quad x_i \in \mathbf{x} \tag{11}$$

Lyapunov's theory can be used in order to compute a control signal that forces the state movement on S:

$$V(\mathbf{x}) = \frac{1}{2}\sigma(\mathbf{x})^2 > 0, \quad \dot{V}(\mathbf{x}) = \dot{\sigma}\sigma \tag{12}$$

Usually, by making proper manipulation, the first derivative of the sliding variable can be expressed as a function of the control variable:

$$\dot{\sigma} = \dot{\sigma}(u) \tag{13}$$

Then, by choosing the following discontinuous control law:

$$u = k_s sign(\sigma) \tag{14}$$

with a sufficiently large k_s, it's possible to guarantee $\dot{V} < 0$.

Note that the 1^{st}-order sliding mode is characterized by a discontinuous control law. When the system reaches the

sliding surface, a chattering phenomenon on the control variable will be triggered at an ideally infinite frequency. This fact entails a very intense use of the control variable and determines the presence of undesired vibrations on the overall system, that can also damage physical components. These phenomena can be reduced, either by approximating the sign function or implementing an higher order SMC.

4.2 A different formulation of the model

In order to design a proper control law, a different formulation of the model has been adopted. Ignoring momentarily deadzone and internal leakages, the valve model can be written as follows:

$$\Phi_1 = S(\nu)\lambda_1^+\sqrt{Pp - P1} + S(-\nu)\lambda_1^-\sqrt{P_1 - P_t} \quad (15)$$

$$\Phi_2 = S(-\nu)\lambda_2^-\sqrt{Pp - P2} + S(\nu)\lambda_2^+\sqrt{P_2 - P_t} \quad (16)$$

$$\lambda_1^- = k_1^-(x_v)\frac{\pi}{4}d^2\sqrt{2/\rho} \quad \lambda_1^+ = k_1^+(x_v)\frac{\pi}{4}d^2\sqrt{2/\rho} \quad (17)$$

$$\lambda_2^- = k_2^-(x_v)\frac{\pi}{4}d^2\sqrt{2/\rho} \quad \lambda_2^+ = k_2^+(x_v)\frac{\pi}{4}d^2\sqrt{2/\rho} \quad (18)$$

$$\nu = f(x_v) = \frac{x_v^2}{\sqrt{(1 - x_v^4)}}sign(x_v) \quad (19)$$

where $S(\nu)$ is the Heaviside step function. Therefore, the flow rates can be expressed as $Q_1 = \Phi_1\nu$ and $Q_2 = \Phi_2\nu$. Also, a new state vector can be defined:

$$\mathbf{z}^t = \begin{pmatrix} e & \dot{e} & P_1 & P_2 \end{pmatrix} = \begin{pmatrix} z_1 & z_2 & z_3 & z_4 \end{pmatrix} \quad (20)$$

where $e = {x_p}^0 - x_p$ and $\dot{e} = \dot{x}_p^0 - \dot{x}_p$ are the position and speed tracking errors, respectively. By defining the following quantities:

$$H_1 = \frac{A_1\Phi_1}{V_1(x_p)} + \frac{A_2\Phi_2}{V_2(x_p)} \quad H_0 = \frac{A_1^2}{V_1(x_p)} + \frac{A_2^2}{V_2(x_p)} \quad (21)$$

z_2 can be expressed as a function of the hydraulic force first derivative:

$$z_2 = \frac{\dot{F}_p}{\beta H_0} - \frac{H_1}{H_0}\nu + \dot{x}_p^0 \quad (22)$$

Finally, the new formulation is obtained by writing (1) with respect to the new state vector:

$$\begin{cases} \dot{z}_1 = \frac{1}{\beta H_0}\dot{F}_p - \frac{H_1}{H_0}\nu + \dot{x}_p^0 \\ \dot{z}_2 = \frac{1}{M}[F_{loss}(\dot{x}_p^0 - z_2) - A_1 z_3 + A_2 z_4 + g + \ddot{x}_p^0] \\ \dot{z}_3 = -\frac{\beta}{V_1(x_p^0 - z_1)}A_1(\dot{x}_p^0 - z_2) + \frac{\beta}{V_1(x_p^0 - z_1)}\Phi_1\nu \\ \dot{z}_4 = -\frac{\beta}{V_2(x_p^0 - z_1)}A_2(\dot{x}_p^0 - z_2) - \frac{\beta}{V_2(x_p^0 - z_1)}\Phi_2\nu \end{cases} \quad (23)$$

where $F_{loss}(\dot{x}_p) = f_r(\dot{x}_p) - D\dot{x}_p - \zeta\dot{x}_p^2$.

4.3 Evaluation of the control law

The design of the control law starts with the definition of a proper sliding variable and a candidate Lyapunov function. A common choice is:

$$\sigma(\mathbf{z}) = C_1 z_1 + z_2, \quad V(\mathbf{z}) = \frac{1}{2}\sigma(\mathbf{z})^2 \quad (24)$$

In order to ensure $\dot{V}(\mathbf{z}) < 0$ the aforementioned control law can be used:

$$\nu = k_s sign(\sigma) \quad (25)$$

Unfortunately with the current experimental set-up the measure of z_2, which depends on $\dot{x}_p$, is not available. However at the increasing of C_1, the dependency of $\sigma(\mathbf{z})$ of z_2 becomes negligible, therefore the time derivative of $V(\mathbf{z})$ can be written as:

$$\dot{V}(\mathbf{z}) = \sigma(z_1)\left[-\frac{C_1 H_1}{H_0}\nu + \frac{C_1\dot{F}_p}{\beta H_0} + C_1\dot{x}_p^0\right] \quad (26)$$

and the control law changes into:

$$\nu = k_s sign(z_1) \quad (27)$$

The numerical value of k_s is computed accordingly to the absolute upper bound of the hydraulic force time derivative(UB_{dF_p}) and reference velocity ($UB_{\dot{x}_p^0}$).

$$k_s > \frac{H_0}{H_1}\left[\frac{UB_{dF_p}}{\beta H_0} + UB_{\dot{x}_p^0}\right] \quad (28)$$

The maximum speed achievable by the load depends on the supply pressure and it can be set as the upper bound of the reference speed. Also both UB_{dF_p} and $UB_{\dot{x}_p^0}$ can be estimated by several simulations of the validated model, as suggested in [21].

In addition, control law (27) can be improved by adding feed-forward and proportional actions:

$$\nu = k_p z_1 + k_s sign(z_1) + \frac{H_0}{H_1}\dot{x}_p^0 \quad (29)$$

therefore the condition on the time derivative of the candidate Lyapunov function becomes:

$$\sigma(z_1)\left[-\frac{H_1}{H_0}(k_p z_1 + k_s sign(z_1)) + \frac{UB_{dF_p}}{\beta H_0}\right] < 0 \quad (30)$$

In order to compute k_s the worst case can be considered. More specifically, the value of the control signal ν is minimum when the proportional action tends to zero ($z_1 \approx 0$), thus the condition on k_s can be re-written as follows:

$$k_s > \frac{UB_{dF_p}}{\beta H_1} \quad (31)$$

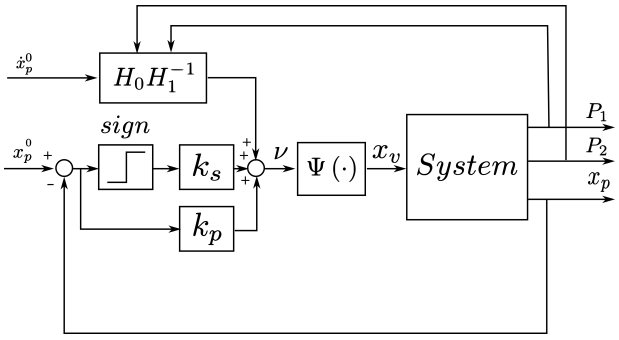

Figure 2. Sliding mode control scheme with proportional term, feedforward model based and sigmoid

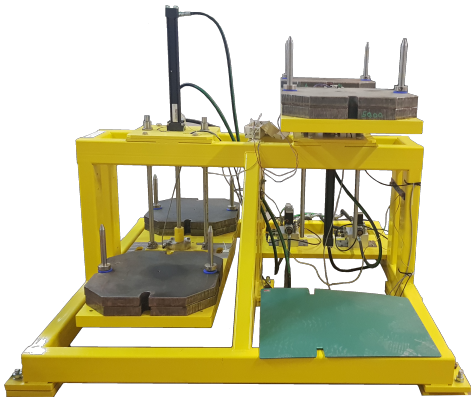

Figure 3. Hydraulic test-bench.

By using the proposed control law (29) a less stringent condition has been retrieved:

$$\frac{UB_{dF_p}}{\beta H_1} \leq \frac{H_0}{H_1}\left[\frac{UB_{dF_p}}{\beta H_0} + UB_{\dot{x}_p^0}\right] \tag{32}$$

Consequently, smaller values of k_s can be adopted and in general smaller oscillations can be induced with respect to the ones determined by control law (27) .

Furthermore, the introduction of the proportional term and of the model-based feed-forward action entails a faster time response and an improvement of the dynamic tracking performances.

Moving to the dead-zone, its effect can be considered by means of a further condition on k_s. In particular, with reference to the worst case, the following condition must be always satisfied:

$$k_s > max\{|f(d_z^+)|, |f(d_z^-)|\} \tag{33}$$

Moreover, in order to reduce the undesired oscillations, triggered by the presence of the $sign(\cdot)$, a sigmoid approximate function is usually adopted:

$$sign(x) \approx sig(x) = -1 + \frac{2}{1 + e^{-\epsilon x}} \tag{34}$$

Finally, once ν is computed, it is possible to find the corresponding valve opening by directly inverting function f:

$$x_v = \Psi(\nu): \quad f(\Psi(\nu)) = \nu \tag{35}$$

The result is a smooth control action at the price of a partial loss in terms of robustness and accuracy (see [21]). Nevertheless, as shown in the next discussion, this choice does not significantly compromise the overall tracking performance.

5 Experimental Validation and Performance Analysis

In this Section the experimental validation platform is described, experimental results are presented, and, finally, the performance levels achieved by each control solution are compared together.

5.1 Hydraulic Test-bench

The hydraulic test-bench used to test the proposed control schemes is pictured in Figure 3. The system is composed by two independent hydraulic servomechanisms. The rod-side of each cylinder is rigidly connected to the load, which consists in a plate (constrained by vertical motion guides) on top of which it is possible to load a generic weight. More in detail, the test-bench comprises:

- 2 asymmetric hydraulic cylinders: one with a traction load and one with a compression load;
- 2 directional valves with 4 ways and 3 positions;
- 1 hydraulic pump powering the entire system;
- pressure relief valves to ensure operational safety;
- 2 linear potentiometers that measure the position of each cylinder;
- 5 pressure sensors installed at the outlet of the pump and inside the four chambers of the two cylinders;
- 2 load cells installed between the rod side and the plate.

5.2 Experimental Validation - Linear Controller

The control scheme pictured in Figure 1 has been tuned in the following way:

$$k_p = 1, \quad k_v = 0.108, \quad T = 0.002, \quad \eta = 50 \tag{36}$$

All the transfer functions have been discretized using the Backward Euler method and the experiments have been

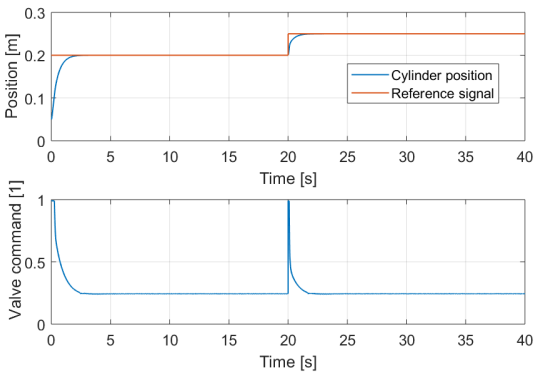

Figure 4. Linear Controller: response to step set-point.

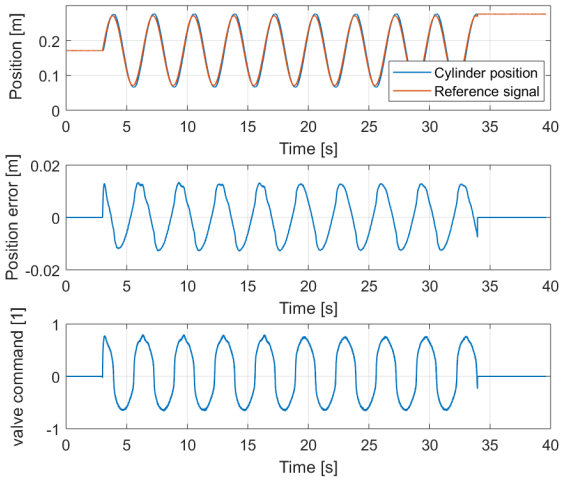

Figure 5. Linear Controller: response to sine reference signal.

performed on the actuator with a compression load mass of 282 kg.

Figure 4 show the system responses to a step set-point. The control action is not affected by any chattering and the system converges to the desired set-point value without oscillating.

On the other hand, Figure 5 shows the results of a tracking experiment during which a sinusoidal reference signal is sent to the control system. The control action seems not to be affected by significant chattering phenomena. Nevertheless, the not completely accurate compensation of the valve dead-zone determines a relevant tracking error, that reaches up to 13.4 *mm* where the sign of the speed changes.

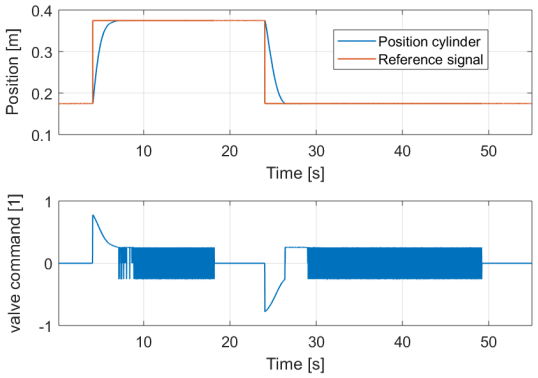

Figure 6. SMC: response to step reference signal.

5.3 Experimental Validation - SMC

At first, a simplified version of SMC law (29) was implemented in the hydraulic test-bench:

$$v = k_p(x_p^0 - x_p) + k_s sign(x_p^0 - x_p) \tag{37}$$

with:

$$k_p = 4.5 \quad k_s = 0.067 \tag{38}$$

The response to a step set-point is shown in Figure 6. The system is able to converge to the imposed set-point with zero static error. Nevertheless, as soon as the state reaches the sliding surface, the control variable starts to chatter at high frequency.

In order to improve the dynamic tracking performance, the feed-forward term was added to equation (37):

$$v = k_p(x_p^0 - x_p) + k_s sign(x_p^0 - x_p) + \frac{H_0}{H_1}\dot{x}_p^0 \tag{39}$$

In addition, to simplify the implementation, the following assumptions have been made:

$$\frac{H_0}{H_1} \approx \frac{A_1}{\Phi_1}, \quad k_1^+ = 0.052, \quad k_1^- = 0.045 \tag{40}$$

Figure 7 shows the response of the system to a sinusoidal reference signal. After the initial peak, the position error rapidly decreases with a maximum of 3.3 *mm*. The chattering phenomenon of the valve opening is still visible. To remove these undesired oscillations, the final SMC law (29) was implemented choosing $\epsilon = 4000$.

Figure 8 shows the response of the complete SMC law to a trapezoidal set-point profile, while Figure 9 shows the response to a sinusoidal reference signal. In both cases, we can see that good performance in terms of position error are achieved (maximum tracking error on sine signal is equal to 6.4 *mm*) and that the use of the approximating sigmoid function enforces a smooth control action, without any significant chattering.

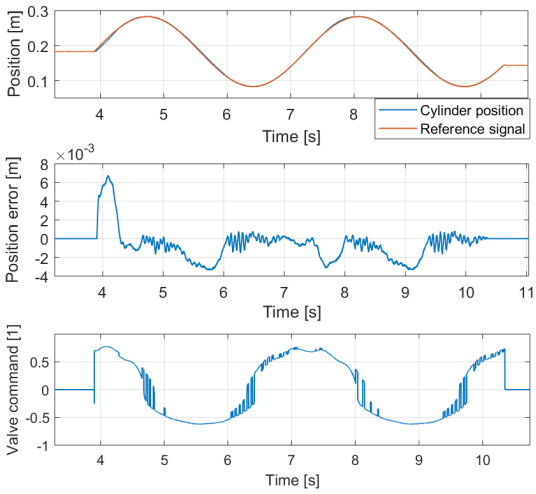

Figure 7. SMC with feedforward: response to sine reference signal.

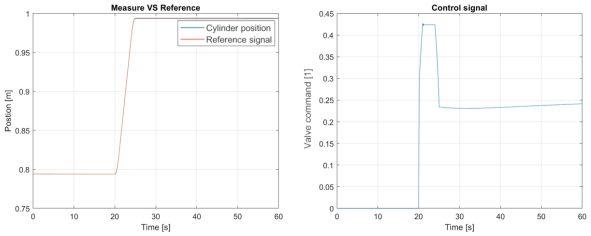

Figure 8. SMC with feed-forward and sigmoid: response to trapezoidal set-point profile.

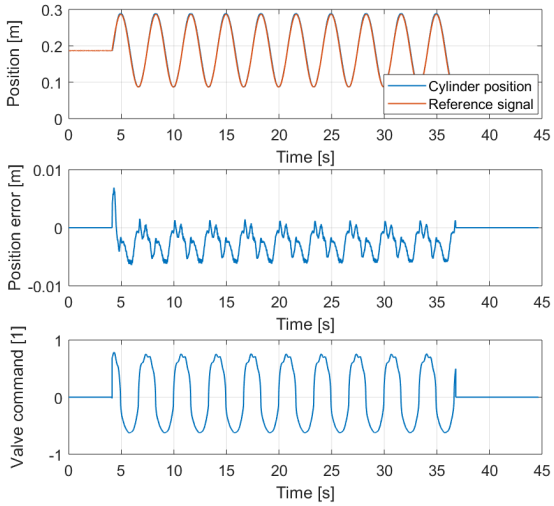

Figure 9. SMC with feed-forward and sigmoid: response to sine reference signal.

5.4 Comparative Evaluation of Performance

Generally, we can state that the linear controller is able to achieve good static performance, but it also entails poor tracking capabilities. Moving to the classical SMC controller, this solution is able to guarantee the best performance both in steady-state and in tracking, but the control action is heavily affected by chattering. Finally, the introduction of the feed-forward term and of the sigmoid approximating function allows to eliminate the chattering problem, without significantly undermining the performance in terms of both convergence time and tracking error.

6 Conclusions and Future Developments

This paper describes the research activities leading to the development of several position control schemes for a standalone hydraulic servomechanism. Starting from a previously validated mathematical model of the hydraulic actuator, several control laws have been synthesized and validated on an real system. Various experiments have been performed in order to verify the performance of each control schemes with respect to both step set-points and sinusoidal reference signals. Experimental results suggest that the SMC schemes (both the classical one and the one with sigmoid approximation) are able to guarantee better performance with respect to the linear cascade control scheme. Moreover, the intrinsic robustness of the SMC strategy leads to a high level of accuracy of the closed loop system.

As far as future developments are concerned, at first a decentralized position control system for an hydraulic manipulator will be designed on the basis of the SMC schemes here discussed. Then, possible alternatives in terms of control strategies will also be evaluated, like for instance the SuperTwisting algorithm (which is an example of 2^{nd}-order SMC) [22], and the linear control with adaptive compensation of the dead-zone [23].

References

[1] M. Hutter, P. Leemann, S. Stevsic, A. Michel, D. Jud, M. Hoepflinger, R. Siegwart, R. Figi, C. Caduff, M. Loher, and S. Tagmann. Towards optimal force distribution for walking excavators. In Advanced Robotics (ICAR), 2015 International Conference on, pages 295–301, July 2015.

[2] M. Tanzini, J. M. Jacinto-Villegas, A. Filippeschi, M. Niccolini, and M. Ragaglia. New nteraction metaphors to control a hydraulic working machine's arm. In IEEE Symposium of Safety and rescue Robotics (SSRR), 2016.

[3] Peter Corke, Jonathan Roberts, Jock Cunningham, and David Hainsworth. Mining Robotics, pages 1127–1150. Springer Berlin Heidelberg, Berlin, Heidelberg, 2008.

[4] John Billingsley, Arto Visala, and Mark Dunn. Robotics in Agriculture and Forestry, pages 1065–1077. Springer Berlin Heidelberg, Berlin, Heidelberg, 2008.

[5] Mohieddine Jelali and Andreas Kroll. Hydraulic servo-systems: modelling, identification, and control. 01 2003.

[6] Torben Andersen, Michael Hansen, Henrik Pedersen, and Finn Conrad. Comparison of linear controllers for a hydraulic servo system. Proceedings of the JFPS International Symposium on Fluid Power, 2005, 01 2005.

[7] Y. Liu and H. Handroos. Technical //note sliding mode control for a class of hydraulic position servo. Mechatronics, 9(1):111 – 123, 1999.

[8] M. Jerouane and F. Lamnabhi-Lagarrigue. A new robust sliding mode controller for a hydraulic actuator. In Proceedings of the 40th IEEE Conference on Decision and Control (Cat. No.01CH37228), volume 1, pages 908–913 vol.1, 2001.

[9] S. Aranovskiy and C. Vazquez. Control of a single-link mobile hydraulic actuator with a pressure compensator. In 2014 IEEE Conference on Control Applications (CCA), pages 216–221, Oct 2014.

[10] Carlos Vazquez, Stanislav Aranovskiy, Leonid Freidovich, and Leonid Fridman. Second order sliding mode control of a mobile hydraulic crane. In Decision and Control (CDC), 2014 IEEE 53rd Annual Conference on, pages 5530–5535. IEEE, 2014.

[11] Rui Tang and Qi Zhang. Dynamic sliding mode control scheme for electro-hydraulic position servo system. Procedia Engineering, 24(Supplement C):28 – 32, 2011.

[12] Cheng Guan and Shanan Zhu. Adaptive time-varying sliding mode control for hydraulic servo system. In ICARCV 2004 8th Control, Automation, Robotics and Vision Conference, 2004., volume 3, pages 1774–1779 Vol. 3, Dec 2004.

[13] Cheng Guan and Shuangxia Pan. Adaptive sliding mode control of electro-hydraulic system with nonlinear unknown parameters. Control Engineering Practice, 16(11):1275 – 1284, 2008.

[14] Lasse Schmidt. Robust Control of Industrial Hydraulic Cylinder Drives - with Special Reference to Sliding Mode- & Finite-Time Control. PhD thesis, Aalborg Universitet, 2014.

[15] Mohammad Reza Sirouspour and Septimiu E Salcudean. Nonlinear control of hydraulic robots. IEEE Transactions on Robotics and Automation, 17(2):173–182, 2001.

[16] Mauro André Barbosa Cunha, Raul Guenther, Edson R. De Pieri, and Victor Juliano De Negri. Design of cascade controllers for a hydraulic actuator. International Journal of Fluid Power, 3(2):35–46, 2002.

[17] Mauro André Barbosa Cunha, Raul Guenther, and Edson R. De Pieri. A fixed cascade controller with an adaptive dead-zone compensation scheme applied to a hydraulic actuator. Control 2004, Bath, United Kingdom, 2004.

[18] Mauro André Barbosa Cunha and Raul Guenther. Adaptive cascade control of a hydraulic actuator with an adaptive dead-zone compensation. In ABCM Symposium Series in Mechatronics, volume 2, pages 385–392, 2006.

[19] Leandro dos Santos Coelho and Mauro André Barbosa Cunha. Adaptive cascade control of a hydraulic actuator with an adaptive dead-zone compensation and optimization based on evolutionary algorithms. Expert Systems with Applications, 38(10):12262–12269, 2011.

[20] Manuel Pencelli, Renzo Villa, Alfredo Argiolas, Gianni Ferretti, Marta Niccolini, Matteo Ragaglia, Paolo Rocco, and Andrea Maria Zanchettin. Accurate dynamic modelling of hydraulic servomechanisms. In Design, Automation and Test in Europe (DATE), 03 2019.

[21] Leonid Fridman Yuri Shtessel, Christopher Edwards and Arie Levan. Sliding mode control and observation. Springer, 2014.

[22] T. Gonzalez, J. A. Moreno, and L. Fridman. Variable gain super-twisting sliding mode control. IEEE Transactions on Automatic Control, 57(8):2100–2105, Aug 2012.

[23] Mauro André Barbosa Cunha, Raul Guenther, and Edson R. De Pieri. A fixed cascade controller with an adaptive dead-zone compensation scheme applied to a hydraulic actuator. Control 2004, Bath, United Kingdom, 2004.